NOVEL DIRECTIONAL SOLIDIFICATION PROCESSING OF HYPERMONOTECTIC ALLOYS

NCC8-209 – Final Report

By

PI: William Kaukler, PhD

Co-Investigator : Alex Fedoseyev

August 17, 2002

Center for Materials Research

The University of Alabama in Huntsville

For

NASA, Marshall Space Flight Center

Dr. Richard N. Grugel
Marshall Space Flight Center
MS – SD46
Huntsville, AL 35812

INTRODUCTION

With the intent of producing uniform composites, solidification processing of hypermonotectic alloys in a microgravity environment began with the 1973 Skylab mission and has continued since. In microgravity, despite the favorable reduction in acceleration, gravity *independent* factors cause coalescence and massive segregation of the liquid phases. This results in a highly inhomogeneous structure. This project would negate these detrimental factors by utilizing ultrasonic energy to initiate and maintain a uniform dispersion of the excess L_{II} phase. An experimental and modeling effort was undertaken with the intent of understanding and optimizing the processing parameters necessary to produce a uniformly aligned hypermonotectic composite during controlled directional solidification.

The binary miscibility gap system of interest is characterized by 1) a region where two distinctly different liquids are in thermodynamic equilibrium and 2) the monotectic reaction, $L_I = S_I + L_{II}$. Microstructural development at the solid/liquid interface for these alloys has been theoretically discussed by Chadwick[1] and Cahn[2] and experimentally investigated by Livingston and Cline[3] and Grugel and Hellawell[4,5].

Alloy compositions to the right of the monotectic reaction are termed hypermonotectic and, upon cooling, pass through the two liquid miscibility gap. Solidification of these alloys for applications as, e.g., slide bearings is hampered by the inherent, usually large, density differences between the L_I and L_{II} phases. This leads to rapid separation, coalescence and, consequently, a highly inhomogeneous structure. It was envisioned that processing in a microgravity environment would eliminate the density differences and a uniform composite of aligned or finely dispersed L_{II} (eventually S_{II}) in the S_I matrix could be produced. Unfortunately, microgravity experiments still resulted in highly macrosegregated structures[6]; ref. 10 lists many papers reporting similar results.

A number of explanations for these poor results have been posed. They include droplet coalescence by Ostwald ripening and/or thermocapillary convection and preferential wetting of the container by one of the liquid phases. These factors, which are both detrimental to microstructure *and* gravity independent, merit consideration here.

Earlier experiments where hypermonotectic alloys were directionally solidified[7-9] served to demonstrate the detrimental effects of phase separation on microstructure. While the above-mentioned coarsening and wetting cannot be eliminated, they may be used to some advantage. It has been shown[10-13] that these gravity independent effects could be accommodated through the inclusion of fibers that served to accrue and uniformly distribute the L_{II}. As the directional

solidification front advances the fibers and adhering L_{II} are uniformly incorporated into the S_I + L_{II} matrix. This process, however, does necessitate fibers.

To this end it is suggested to apply an ultrasonic field to the bulk liquid that, upon cooling, will initiate and maintain a uniform dispersion of the precipitated liquid, L_{II}. The microgravity environment would then serve to eliminate density differences, i.e., settling, between the liquids. With droplet coalescence minimized, controlled directional solidification should promote a uniformly aligned, composite microstructure.

The study of acoustic waves on initiating and maintaining suspensions in two-liquid systems is well established. In 1927 Wood and Loomis[14] reported using high-frequency sound waves of great intensity to form emulsions. Shortly after, Richards[15] used lower intensities of sound and was able to emulsify many liquid immiscibility systems. Mechanisms for emulsification by ultrasonic waves were further investigated in a series of papers published in the 1930's by Sollner, *et al.*[16] and they were able to emulsify a maximum of 6g mercury in 1 liter of water. Schmid *et al.*[17] (late 1930's) applied ultrasonics to a number of pure metal and alloy melts. Overall, upon solidification, a comparatively much finer microstructure resulted. They also produced a dispersion of lead in the immiscible aluminum-lead system that was considerably finer at the top. A number of papers reporting the results of applying ultrasonic energy to solidifying melts have since been published [e.g. 18-26]; again overall finer and more uniform microstructures resulted.

Clancy et al., realizing the need for a uniform distribution of droplets and/or particles prior to solidification processing in a microgravity environment, developed an ultrasonic mixing system for use with existing Spacelab furnace hardware[27]. Subsequently, microstructural examination of a hypermonotectic zinc - 5 wt pct lead alloy, (microgravity environment provided by TEXUS sounding rockets) showed a better distribution of the Pb-phase with acoustics applied than without[28,29]. In a similar microgravity experiment, Takahashi et al.[30] solidified hypermonotectic aluminum - 30 wt pct indium alloys subjected to ultrasonic energy; again considerably better dispersions were found.

The above experiments examined metallic, miscibility gap systems from which microstructural development must be inferred after solidification is complete. Using transparent materials that simulate solidification phenomena in metals and alloys, a well-established technique[31], may circumvent this hindrance.

PRELIMINARY EXPERIMENTAL ASPECTS

With reference to the succinonitrile - glycerol phase diagram, Fig. 1, consider the following demonstration[32].

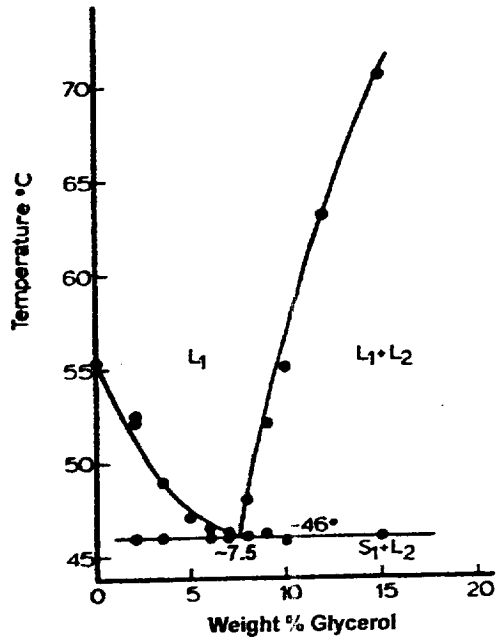

Fig. 1 Partial Succinonitrile - Glycerol phase diagram[33].

Hypermonotectic succinonitrile - 15 wt pct glycerol "alloys" were made and placed in 12mm I.D test tubes. The samples were instrumented with a thermocouple and submerged in the water bath of a commercial ultrasonic cleaner, the initial bath temperature being ~90°C. When the bath, and sample, cooled to ~73°C precipitation of the excess L_{II} phase (glycerol) initiates. After 45 minutes, ~51°C, the coalesced glycerol fully occupies the sample bottom, Figure 2 - left. Subsequent solidification results in a highly segregated structure. The right side of Fig. 2 shows a similar sample that was subjected to ultrasonic energy during cooling. At ~50 °C and 105 minutes, after precipitation of the L_{II} phase initiated, a uniform dispersion of the excess liquid is maintained.

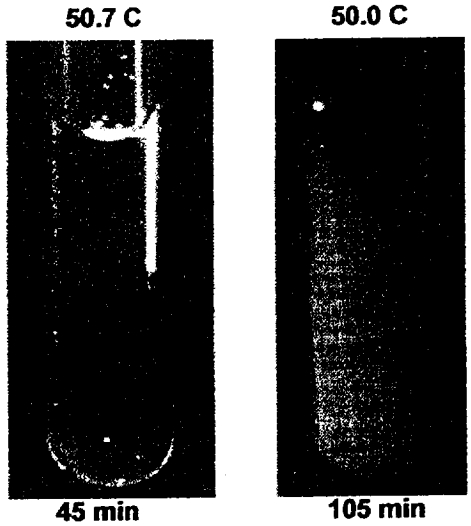

Fig. 2 Left: Settling and coalescence of L_{II} (glycerol) as the sample cools through the miscibility gap. Right: L_{II} droplets remain suspended in an ultrasonic field.

Controlled directional solidification experiments generally consider four processing parameters, i.e., growth rate (V), temperature gradient (G), composition (C_o), and gravity (g). Applying ultrasonics introduces many additional variables. These include frequency, amplitude, sample dimensions, heat generation, and melt-probe interactions and must be considered.

A schematic representation of the directional solidification apparatus used in this investigation is depicted in Figure 3a. A photograph of this apparatus is shown in Fig 3b. This shows the peripheral support electronics as well. Here the sample and probe are fixed with the heating-cooling units translated at the desired rate. The heater consists of a resistance winding (~1cm intervals) around a quartz tube that permits direct observation and video recording of events at the solid/liquid interface.

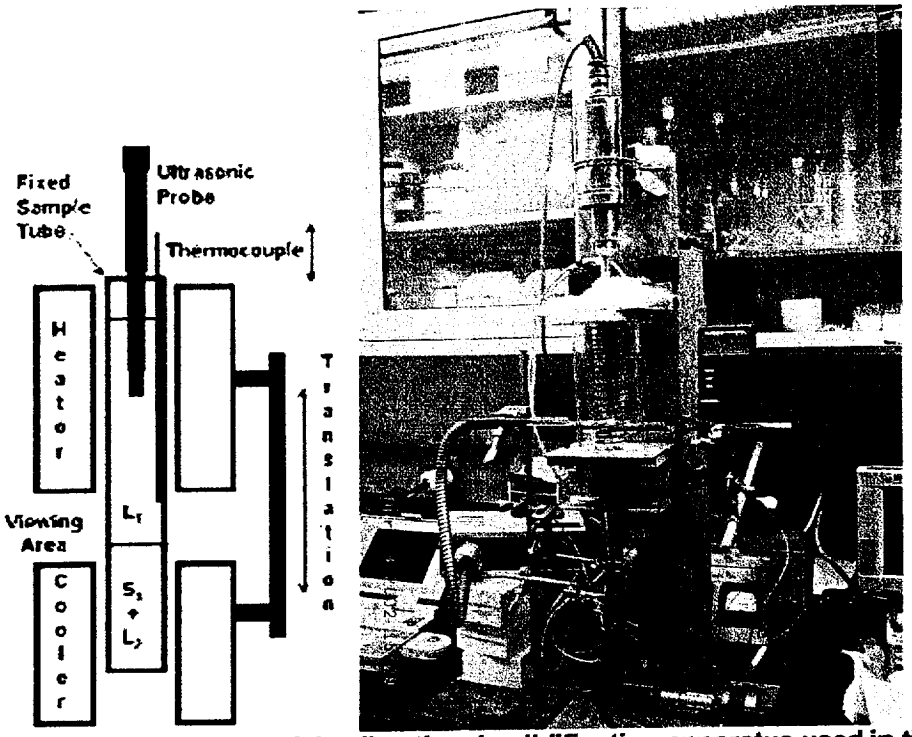

Fig. 3a Schematic representation of the directional solidification apparatus used in this investigation.
Fig. 3b Photograph of the apparatus in Dr. Grugel's laboratory.

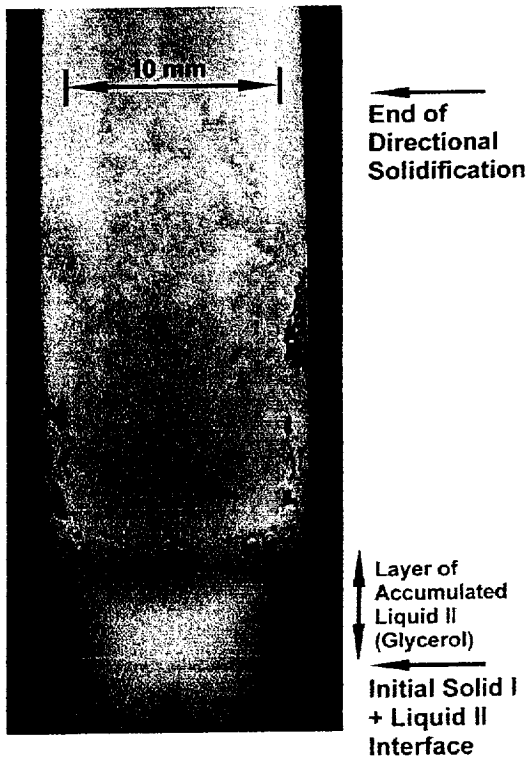

Fig. 4a Macrograph of a Succinonitrile - 15 wt pct Glycerol "alloy" directionally solidified at $5\mu ms^{-1}$. The layer of $Liquid_{II}$ (glycerol) forms during melting prior to reaching equilibrium. Note that the sample tube is 12mm OD, 10mm ID.

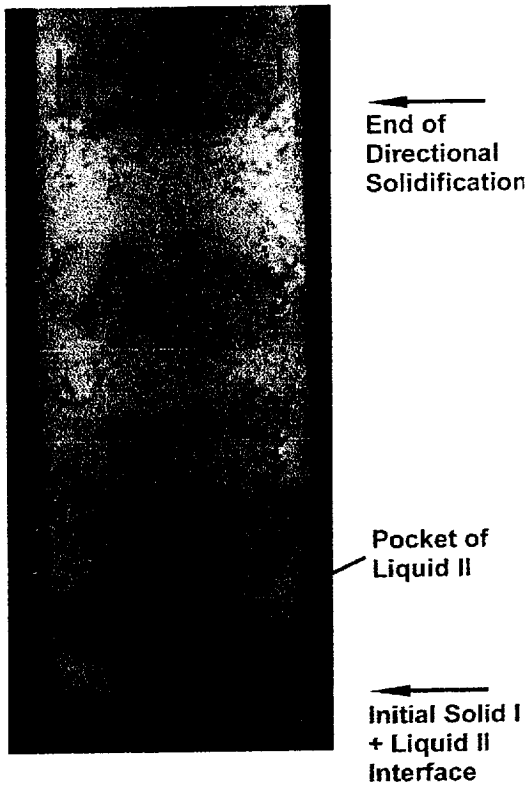

Fig. 4b Improved microstructural uniformity as a consequence of applying ultrasonic (f = 20 kHz) energy with a probe amplitude of 137μm for 0.1 second/second during controlled directional solidification.

The macrostructure of a hypermonotectic "alloy" which has been directionally solidified in the above-mentioned furnace is shown in Figure 4a. Clearly visible is a layer of excess, denser, L_{II} that has accumulated at the (now) equilibrium $S_I + L_{II}$ interface as established by the temperature gradient. From observation, the layer of glycerol initially forms once the sample is placed into the furnace. Initially, as it heats up, the mixture passes through the two liquid region prior to reaching an equilibrium L_I temperature. During this time precipitated L_{II} can sink and accumulate. Secondly, it takes time for the $S_I + L_{II}$ interface to stabilize. As it slowly melts back and passes through the miscibility gap the denser glycerol contributes to the L_{II} layer. Conversely, the less dense succinonitrile-rich L_I develops under the L_{II} layer until a sufficient mass is developed which then releases, passes through the layer, and contributes to the upper bulk liquid. Obviously, this process compromises the desired microstructural homogeneity.

In contrast, Figure 4b shows an identical sample that was directionally solidified in the presence of an applied ultrasonic field. Here only a small pocket of L_{II} accumulated at the $S_I + L_{II}$ interface. The horizontal banding is a result of manually moving the probe tip in relation to the advancing interface. It is envisioned that the observed L_{II} pocket can be further minimized

(or eliminated) by optimizing the processing parameters. Modifying the experimental apparatus such that the probe moves in conjunction with the heating and cooling units will control banding. Further work involves scaling and applying the processing parameters to a metallic sample from which microstructural and compositional analysis will be facilitated.

Experiments and Model Development

In addition to other factors, gravity driven separation precludes uniform microstructural development during controlled directional solidification (DS) processing of immiscible, hypermonotectic, alloys [3, 4]. This is characteristic of metal systems that exhibit a region of liquid-liquid immiscibility and upon cooling tend to separate much as an oil and vinegar salad dressing. It is well established that liquid/liquid suspensions, in which the respective components are immiscible and have significant density differences, can be established and maintained by utilizing ultrasound. However, it has not been demonstrated that the process can be applied during controlled directional solidification processing. Figure 5 shows a series of (immiscible) Succinonitrile – Glycerol "alloys" directionally solidified at $5\mu ms^{-1}$ [34]. Clearly seen in each sample is a (dark) layer of liquid glycerol that precipitated and sank to the initial solid/liquid interface during the remelting process. The layer thickness obviously increases with increasing volume fraction of glycerol.

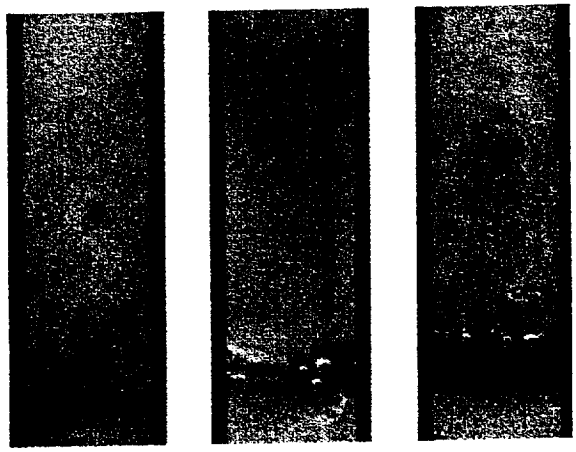

Figure 5

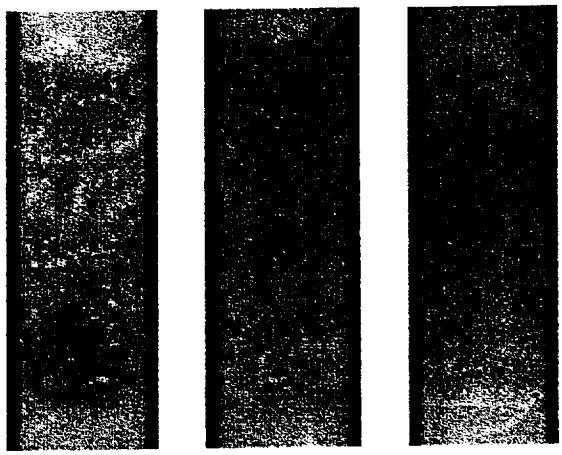

Figure 6

Figure 6 depicts a series of samples subjected to ultrasonic energy using and shows the effect of increasing amplitude on promoting microstructural uniformity in a Succinonitrile – 15-wt pct Glycerol "alloy". (Growth velocity, V, = 5 μms^{-1}, Frequency = 20kHz, Pulse duration = 0.3sec / sec, Tip position = 3.5cm from interface, Sample tube is 12 mm OD, 10mm ID). We note, that the droplet size is smaller, when the amplitude of probe vibration is increased, and that the sedimentation time (when vibration is stopped) is significantly increased when compared alloys not ultrasonically processed.

While the Succinonitrile-Glycerol "alloys" well serve for demonstration, they have no practical commercial value. The intent here is to study and model this system with the goal of scaling to viable products such as bearing alloys and novel superconducting composites where density difference phase separation is a problem. To this end the following approach has been initiated.

Mathematical Model and Numerical Investigation

We consider the ultrasonic field in an experimental ampoule of length $L=0.1m$ and diameter $D=0.01m$ induced by a probe having a vibration frequency of $f=20Khz$ (circular frequency $\omega = 2\pi f$). The amplitude is adjustable from $A=65$ *to* $130\mu m$. The probe tip diameter is $d=0.003m$, the liquid has a density of $\rho = 10^3 Kg/m^3$ in which the speed of sound and surface tension are, respectively, $c = 1.904m/s$ and $\sigma = 4 \cdot 10^{-2} N/m$. These are representative numbers for organic materials. More precision will be shown in the calculations shown at the end of this document.

The radii, R, of the "Liquid II" droplets are estimated using an energy approach. The sound pressure amplitude at the vibrating flat probe surface tip is $P_A=\rho\, cA\, \omega$, and for our case the magnitude of P_A is P_A =24Mpa = 240Atm. The sound pressure far from the probe tip (at distances >> *d*, assuming a plane wave front) is of the order $p_a=P_A(d/D)^2$, so the magnitude of the sound pressure in our case is $p_a=2.4\ Mpa$.

To derive the scale of the stable droplet size of Liquid II we use the following assumptions:

(i) The droplet size is small in comparison to the sound wave length ($\lambda = c/f = 0.1m$).

(ii) The forces between droplets are neglected (relative concentration is small).

(iii) The droplet is stable because the kinetic energy, E_K, of the liquid motion due to ultrasonic field influence is less then the binding energy, E_S, due to the surface tension. (It is easy to show that the surface energy of two droplets resulting from one is larger by about a factor of two.)

(iv) The stability limit (characterized by an average observed droplet size) is defined by $E_S = E_K$.

(v) The ultrasonic energy dissipation in the droplets due to viscosity is neglected.

We make the following estimations.

(a) Kinetic energy of the liquid motion in the droplet

The droplet exhibits periodical isotropic elastic compression and expansion due to the sound waves (i.e., assumption (i). The sound itself is a manifestation of the elastic continuum, and the speed of sound is defined as $c=\sqrt{(B/\rho)}$, where B is bulk elastic modulus of the liquid. Maximum relative compression of the liquid volume, by definition, is: $\delta V/V=p/B$, where *V* is the droplet volume, and *p* is a pressure magnitude in the sound wave. The elastic energy gained due to this compression is $E_P = p\delta V = p^2V/B = (4/3)\pi R^3p^2/(\rho c^2)$. The kinetic energy of liquid motion is of the same scale, $E_K = E_P$, if we use assumption (v) above.

(b) The surface energy, by definition, due to the surface tension, is $E_S = 4\pi R^2\sigma$. Using assumption (iv) we obtain the following equation for the radius, *R*:

$$4\pi R^2\sigma = (4/3)\pi R^3p^2/(\rho c^2)$$

and, therefore, the maximum stable radius is $R = 3\sigma\rho c^2/p^2$. Substituting the above value for sound pressure, $p = p_a$ we obtain the maximum stable droplet radius as:

$$R = 3\sigma/(\rho A^2\omega^2)(D/d)^4.$$

The above formula qualitatively describes, as shown in the next section, results from experimental observations of processed Succinonitrile-Glycerol "alloys" and tin dispersions generated in a salt flux.

The calculated glycerol droplet size for the ultrasound processed Succinonitrile-Glycerol "alloys" versus amplitude is presented in Fig. 7a, and the droplet sedimentation velocity versus amplitude *A* is shown in Fig. 7b.

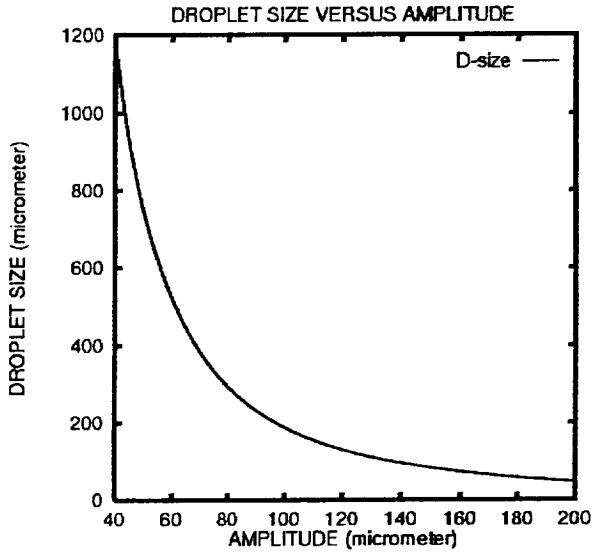

Figure 7a

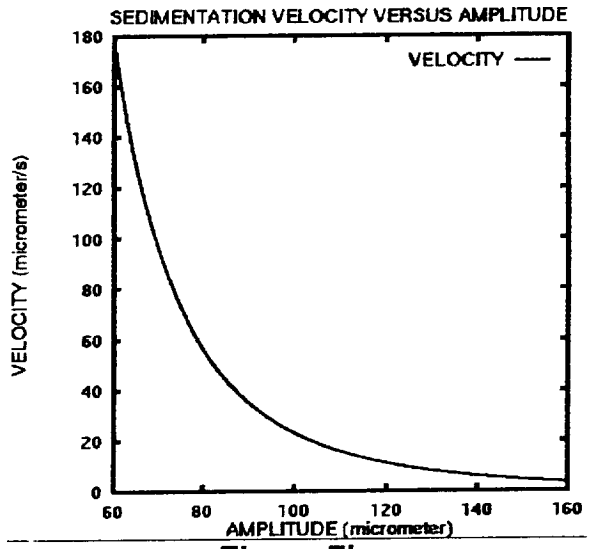

Figure 7b

Figure 7: (a) Liquid II (glycerol) droplet diameter and (b) sedimentation velocity as a function of amplitude *A* for 20kHz.

In view of Figures 7a and b consider the following experimental observations. Figures 4a and b are scanning electron micrographs of tin droplets that were generated from an initially molten mass in a salt flux through application of ultrasonic energy (20 kHz) having a probe amplitude of, respectively, 64 and 137microns.

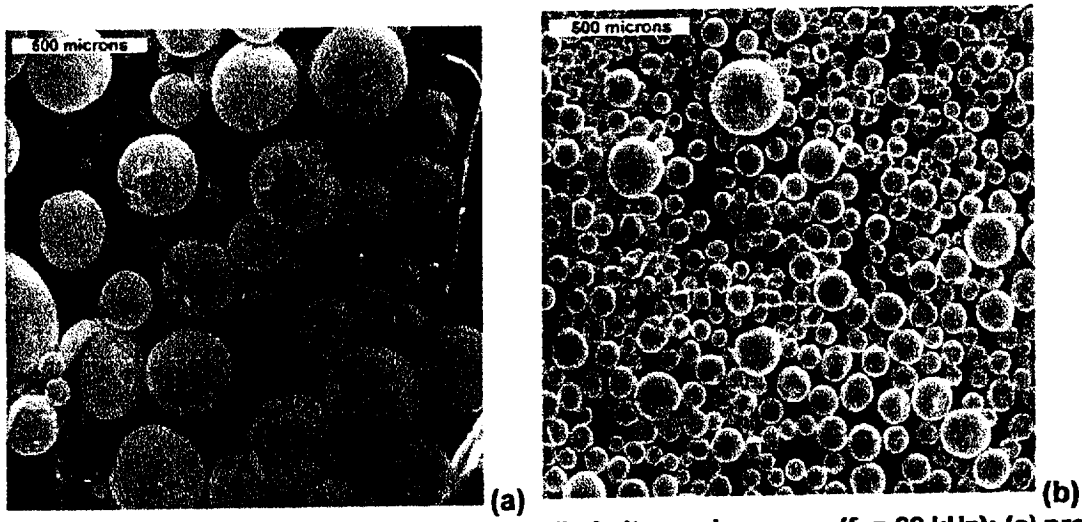

Figure 8: Tin droplet dispersion resulting from applied ultrasonic energy (f = 20 kHz): (a) probe amplitude 64 μm, and (b) 137 μm [36].

It is acknowledged that there is variation in the droplet size for a given processing condition. However, as can be easily ascertained and in accordance with the model, processing tin with about twice the amplitude, *A*, resulted in approximately a four times smaller droplet size. Furthermore, the average particle diameter determined from Figures 8a and b scales well with Figure 7a. Secondly, with regard to Figure 6, the glycerol droplet diameters for the samples processed with amplitudes of 64, 101, and 137 microns are, respectively, ~580, ~200, and ~105 microns. In terms of Figure 7b, this translates to sinking velocities of, respectively, ~170, ~25, and ~6 microns/second. The samples in Figure 6 were being directionally solidified at a rate of 5 microns/second. In the first two cases the settling velocity is much greater than the solidification rate and droplet coalescence (pockets of glycerol) is seen; in the third case the rates are about the same and coalescence is not apparent leading to the suggestion of establishing a steady-state condition of droplet generation/incorporation.

On the following pages are Mathcad calculations (Kaukler) using the derived equations above and independently obtained literature values for the relevant parameters. These were made to verify equations (derived by Fedoseyev and Grugel) and reproduce their conclusions to extend the concepts to new materials combinations.

Mathcad Calculations for Ultrasonic processing of immiscible alloys

Relevant Materials Properties

Sodium Nitrate/ 2%Sodium Chloride Eutectic - Indium or Tin

$\rho_{SN} := 1.906 \frac{gm}{cm^3}$

use properties of molten sodium nitrate, In and Sn shown as T

$\eta_{SN} := 3.047 10^{-3} \cdot Pa \cdot s$

$\sigma_{SN} := 116.4 10^{-3} \cdot \frac{N}{m}$

$\rho_{In} := 7.023 \frac{gm}{cm^3}$

$\rho_T := 7.0 \frac{gm}{cm^3}$

$\sigma_{In} := 0.556 \frac{J}{m^2}$

$\sigma_T := 0.560 \frac{J}{m^2}$

Succinonitrile-15 w% Glycerol

$\rho_{SCN} := 0.988 \frac{gm}{cm^3}$ $\eta_{SCN} := 2.6 10^{-3} \cdot Pa \cdot s$ density & viscosity of liquid SCN at mp

$\rho_G := 1.2613 \frac{gm}{cm^3}$

$\sigma_{SCNG} := 0.0020 \frac{J}{m^2}$ interfacial tension estimated as that between SCN liquid & solid

---

calculated speed of sound for water

$c := \sqrt{\frac{B}{\rho_w}}$

$c = 1.483 \times 10^3 \frac{m}{s}$

Speed of sound in liquids m/s:
water 1497
methyl alcohol 1123
glycerol 1923 or 1904 depends on ref.
mercury 1440

Equipment related parameters

$L := 0.1 \cdot m$ L, length or height of liquid colum

$d := 0.003 \cdot m$ d, diameter of ultrasonic probe tip

$D := 0.01 \cdot m$ D, diamter of inside of ampoule or diameter of fluid column

$f := 20 \cdot 10^{3} \cdot s^{-1}$ f, frequency of ultrasonic system, fixed

$\omega := 2 \cdot \pi \cdot f$ ω, angular frequency of system

$c := 1.4 \cdot 10^{3} \cdot \frac{m}{s}$ c, speed of sound in melt

$\lambda := \frac{c}{f}$ λ, wavelength of sound waves.
Assume droplet size is of same order as this. $\lambda = 0.07m$

$i := 1, 2 .. 100$

$A_i := (50 + i) \cdot 10^{-6} \cdot m$ A, amplitude of probe oscillations, experimentally 65-130 μm

Calculations

Radii calculation for SCN - Glycerol system

$$P_{A_i} := \rho_{SCN} \cdot c \cdot A_i \cdot \omega$$

$$p_{a_i} := P_{A_i}\left(\frac{d}{D}\right)^2$$

$$R_{G_i} := \frac{3 \cdot \sigma_{SCNG}}{\left[\rho_G \cdot (A_i)^2 \cdot \omega^2\right]\left(\frac{D}{d}\right)^4}$$

$$R_{G_i} := 3 \cdot \sigma_{SCNG} \cdot \rho_G \cdot \frac{(c)^2}{\left[\rho_{SCN} \cdot c \cdot A_i \cdot \omega \cdot \left(\frac{d}{D}\right)^2\right]^2}$$

maximum stable radius

$R_{G_1} = 23.303\text{um}$

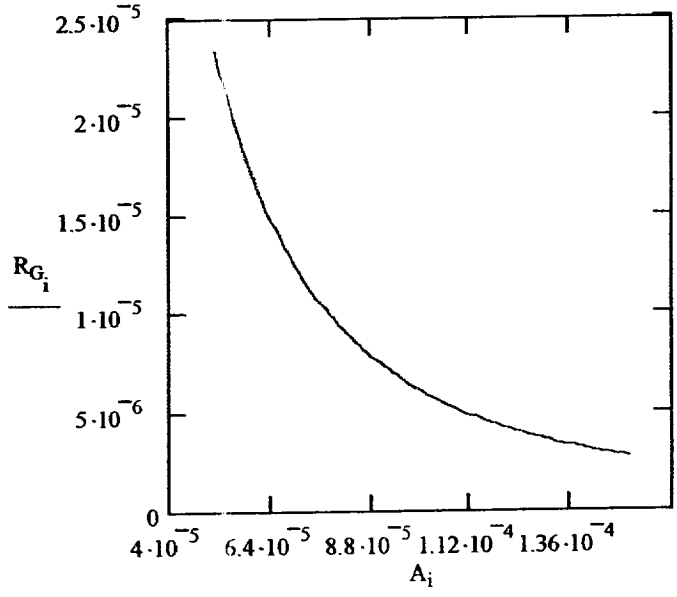

Radii calculation for Tin in Sodium Nitrate Eutectic with Sodium Chloride

$$P_{A_i} := \rho_{SN} \cdot c \cdot A_i \cdot \omega$$

$$p_{a_i} := P_{A_i} \left(\frac{d}{D} \right)^2$$

$$R_{T_i} := 3 \cdot \sigma_T \cdot \rho_T \cdot \frac{(c)^2}{\left[\rho_{SN} \cdot c \cdot A_i \cdot \omega \cdot \left(\frac{d}{D} \right)^2 \right]^2}$$

maximum stable radius

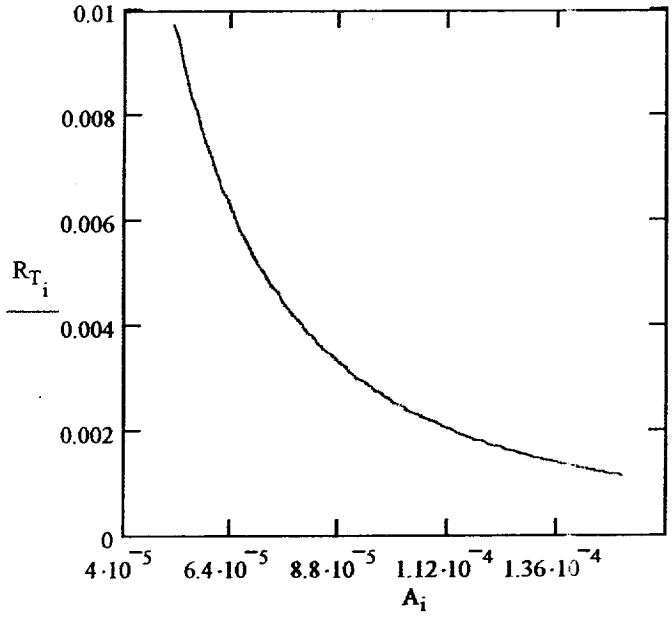

$R_{T_1} = 9.73 \times 10^{-3}$ m

Conclusions

A model has been developed that determines the size of $Liquid_{II}$ droplets generated during application of ultrasonic energy (as a function of amplitude) to immiscible alloys. The initial results are in accordance with experimental results based on Succinonitrile – Glycerol "alloys" and pure tin dispersions. Future work will take into account the importance of other effects, e.g., thermo-vibrational convection [35, 36], sound attenuation, viscosity variations, and compositional changes.

References

1. G.A. Chadwick: *Brit. J. Appl. Phys.*, **16** (1965) 1095.
2. J.W. Cahn: *Metall. Trans. A*, **10A** (1979) 119.
3. J.D. Livingston and H.E. Cline: *Trans. TMS-AIME*, **245** (1969) 351.
4. R.N. Grugel and A. Hellawell: *Metall. Trans. A*, **12A** (1982) 669.
5. R.N. Grugel and A. Hellawell: Materials Research Soc., Proc., Vol. 19, Elsevier, (1982) 417.
6. T. Carlberg and H. Fredriksson: *Metall. Trans. A*, **11A** (1980) 1665.
7. R.N. Grugel, T.A. Lograsso, and A. Hellawell: Materials Processing in the Reduced Gravity Environment of Space, Elsevier, (1982) 553.
8. S. Shah et al: *Metall. Trans. A*, **19A** (1988) 2677.
9. R.N. Grugel and Shinwoo Kim: *Adv. in Space Research*, **13** (1993) 225.
10. R.N. Grugel: *Metall. Trans. B*, **22B** (1991) 339.
11. R.N. Grugel and S. Nourbakhsh: AIAA Paper No. 92-0352, (1992).
12. R.N. Grugel and S. Nourbakhsh: 4th International Symposium, Experimental Methods for Microgravity Materials Science Research, TMS, (1992) 81.
13. R.N. Grugel: U.S. Patent No. 5,246,508, (1993).
14. R.W. Wood and A.L. Loomis: *Phil. Mag.*, **7** (1927) 417.
15. W.T. Richards: *J. Amer. Chem. Soc.*, **51** (1929) 1724.
16. K. Sollner et al.: *Kolloid-Zeit*, **60** (1932) 263; *Trans. Faraday Soc.*, **31** (1935) 835; *Ibid*, **31** (1935) 843; *Ibid*, **32** (1936) 556; *Ibid*, **32** (1935) 616.
17. G. Schmid et al.: *Zeit. Fur Elecktrochem*, **43** (1937) 869; *Zeit. fur Elecktrochem*, **45** (1939) 769; *Zeit. fur Elecktrochem*, **46** (1940) 87.
18. A.H. Freedman and J.F. Wallace: *Trans. Amer. Foundryman's Soc.*, **65** (1957) 578.
19. D.H. Lane, et al: *Trans. AIME*, **218** (1960) 985.
20. D.H. Lane, and W.A. Tiller: *Trans. AIME*, **218** (1960) 991.
21. M. Weinstein: *Trans. AIME*, **230** (1964) 321.
22. H.E. Bates and M. Weinstein: *J. Electrochem. Soc.*, **112** (1965) 693.
23. H.E. Bates and M. Weinstein: *J. Electrochem. Soc.*, **114** (1967) 259.
24. J.A. Bailey and J.R. Davila: *J. Inst. Metals*, **97** (1969) 248.
25. Y. Hayakawa, Y. Sone, K. Tatsumi, and M. Kumagawa: *Japan. J. Appl. Phys.*, **21** (1982) 1273.
26. W. Fengquan, C. Shiyu, H. Deping, W. Bingbo, and S. Guangji: *J. Materials Sci.*, **29** (1994) 3997.
27. P.F. Clancy,et al: *Acta Astronautica*, **7** (1980) 877.
28. P.F. Clancy, W. Heide, and D. Langbein: 4th European Symposium on Materials Science under Microgravity, ESA SP-191 (1983) 99.
29. P.F. Clancy, and W. Heide: Workshop on the Effect of Gravity on Solidification of Immiscible Alloys, ESA SP-219 (1984) 73.
30. T. Takahashi, et al: *J. Japan Inst. Light Metals*, **34** (1984) 479.
31. R.N. Grugel and R. Trivedi: Metallography: Past, Present, and Future (75th Anniversary Volume), ASTM STP 1165, (1993) 393.
32. R.N. Grugel: Unpublished research, Vanderbilt University, 1994.
33. R.N. Grugel: Ph.D. Thesis, Michigan Technological University (1983).
34. R. N. Grugel and S. Kim, Utilizing vibrations to promote uniform composite growth during directional solidification of hypermonotectic alloys: J. Japan. Soc. Microgravity Appl., **15** (1998) 530-536
35. A. I. Fedoseyev and J. I. D. Alexander, Investigation of vibrational control of convective flows in Bridgman melt growth configurations. J. Cryst. Growth, (2000) (to appear)
36. A. I. Fedoseyev, J. I. D. Alexander, An Inverse Finite Element Method for Pure and Binary Alloys. J. Comp. Physics, **130** (1997) 243-255.